LATAM Revista Latinoamericana de Ciencias Sociales y Humanidades, Asunción, Paraguay.
ISSN en línea: 2789-3855, 2025, Volumen VI

Cardiac pulse detection by a pulse train using the synchronous demodulation technique

Detección del pulso cardíaco mediante un tren de pulsos utilizando la técnica de demodulación síncrona

Javier Yañez Mendiola
jyanez@ciatec.mx
https://orcid.org/0000-0003-0772-5947
Ciatec A.C.
León Gto. – México

Roxana Zaricell Bautista López
thaleth0.0@gmail.com
https://orcid.org/0000-0002-3180-8825
Universidad Virtual de Guanajuato
León Gto. – México

José Martin López Vela
lopez2martin@aim.com
https://orcid.org/0009-0000-6261-2473
Investigador Independiente
León Gto. – México

DOI: https://doi.org/10.56712/latam.v6i5.4749

Artículo recibido: 12 de julio de 2025
Aceptado para publicación: 11 de noviembre de 2025.
Conflictos de Interés: Ninguno que declarar.

5
Redilat
Red de Investigadores Latinoamericanos
NÚMERO

DOI: https://doi.org/10.56712/latam.v6i5.4749

Cardiac pulse detection by a pulse train using the synchronous demodulation technique

Detección del pulso cardíaco mediante un tren de pulsos utilizando la técnica de demodulación síncrona

Javier Yañez Mendiola[1]
jyanez@ciatec.mx
https://orcid.org/0000-0003-0772-5947
Ciatec A.C.
León Gto. – México

Roxana Zaricell Bautista López
thaleth0.0@gmail.com
https://orcid.org/0000-0002-3180-8825
Universidad Virtual de Guanajuato
León Gto. – México

José Martin López Vela
lopez2martin@aim.com
https://orcid.org/0009-0000-6261-2473
Investigador Independiente
León Gto. – México

Artículo recibido: 12 de julio de 2025. Aceptado para publicación: 11 de noviembre de 2025.
Conflictos de Interés: Ninguno que declarar.

Abstract

Photoplethysmography is a widely studied noninvasive optical technique with great potential for application in clinical medicine. There is evidence that the PPG signal can provide information about heart rate, oxygen saturation in arterial blood, respiratory rate among other cardiovascular signs. The two-wavelength photoplethysmographic signal is generally used to determine oxygen saturation in arterial blood under the principle that oxygenated and deoxygenated hemoglobin differentially absorb red and near-infrared wavelengths. In this work it is proposed to use the same wavelengths that are used in the pulse oximetry technique (660 nm and 940 nm) to calculate heart rate; Heart rate recovery is done by analyzing the data using the synchronous demodulation technique. The sampled data was generated from measurement carried out on two people. The heart rate obtained with the pulse oximetry technique in conjunction with the synchronous demodulation technique was corroborated with the heart rate obtained using the PPG signal at a single wavelength (940 nm).

Keywords: cardiac pulse, photoplethysmography, sensor, synchronous demodulation

Resumen

La fotopletismografía es una técnica óptica no invasiva ampliamente estudiada con gran potencial de aplicación en la medicina clínica. Existe evidencia de que la señal PPG puede proporcionar información sobre la frecuencia cardíaca, la saturación de oxígeno en sangre arterial y la frecuencia respiratoria, entre otros signos cardiovasculares. La señal fotopletismográfica de dos longitudes de

[1] Autor de correspondencia.

onda se utiliza generalmente para determinar la saturación de oxígeno en sangre arterial, según el principio de que la hemoglobina oxigenada y desoxigenada absorben de forma diferencial las longitudes de onda del rojo y del infrarrojo cercano. En este trabajo, se propone utilizar las mismas longitudes de onda que se emplean en la técnica de oximetría de pulso (660 nm y 940 nm) para calcular la frecuencia cardíaca. La recuperación de la frecuencia cardíaca se realiza mediante el análisis de los datos mediante la técnica de demodulación sincrónica. Los datos muestreados se generaron a partir de mediciones realizadas en dos personas. La frecuencia cardíaca obtenida con la técnica de oximetría de pulso junto con la técnica de demodulación sincrónica se corroboró con la frecuencia cardíaca obtenida mediante la señal PPG a una sola longitud de onda (940 nm).

Palabras clave: pulso cardíaco, fotopletismografía, sensor, demodulación sincrónica

Cómo citar: Yañez Mendiola, J., Bautista López, R. Z., & López Vela, J. M. (2025). Cardiac pulse detection by a pulse train using the synchronous demodulation technique. *LATAM Revista Latinoamericana de Ciencias Sociales y Humanidades 6 (5), 2415 – 2423. https://doi.org/10.56712/latam.v6i5.4749*

INTRODUCTION

Photoplethysmography (PPG) is an optical measurement technique that is used to measure blood volume changes in microvascular tissue (Challoner y Ramsay 1974) and has a wide range of clinical applications, for example, pulse oximetry and cardiac pulse signals. PPG signals have great potential for the non-invasive detection of a wide range of diseases with high performance; in a review of 43 studies that used photoplethysmography (PPG) signals for the detection and diagnosis of 25 health conditions, Loh et al. (Loh et al. 2022) identified some limitations in the studies reviewed, such as the lack of standardization in the collection of PPG signals, the lack of public access to PPG databases, and the diversity of health conditions covered. This review also highlights the importance of noting that PPG studies are still in an early stage of development and that more studies are needed to validate the results obtained and to evaluate the performance of PPG techniques in real clinical settings.

The optical arrangement used is very simple: a light source illuminates the skin and after interacting with the skin either by transmission or reflection, the results are collected for processing. The interaction of light with living tissue is somewhat complex (reflection, transmission, absorption and scattering) (Anderson y Parrish 1981) and many factors affect the amount of light received by the sensor, for example the effect of pressure on the sensor (Hertzman 1938). Although the signal processing technique through the plethysmography method is well known, where for the general case of obtaining a cardiac pulse, a single light source is used; for pulse oximetry, a technique derived from the application of photoplethysmography, two light sources at different wavelengths are used to determine the percentage of oxygen between the proportions of hemoglobin and oxyhemoglobin. (de Kock y Tarassenko 1993; Wukitsch et al. 1988; Chan, Chan, y Chan 2013). Leppänen et al. (Leppänen et al. 2022) indicate that total absorption is lower with infrared light compared to red light, so the PPG signal measured with the infrared wavelength is more stable and commonly used than red light. However, measurements of both red and infrared light are required to estimate SpO2. The main advantage of this device is that data collected from the two different wavelengths can be used to estimate both heart rate and SpO2. Therefore, we propose that by using the pulse oximetry configuration and synchronizing the activation of the light source (red and infrared LEDs) so that the signal sent is a series of pulses, the cardiac pulse signal can be recovered by processing the data using synchronous demodulation technique. Oximetry is a widely studied technique with clinical applications. One of the main applications of pulse oximetry is the determination of oxygen saturation using different signal processing techniques, however, blood oxygen saturation is not the only information that the PPG signal can contain, but also signals of interest such as heart rate and respiratory rate (Chon, Dash, y Ju 2009). It can be shown that it is possible to recover the respiratory rate from the photoplethysmography signal because there is evidence that the respiratory rate modulates both the frequency and the amplitude of the cardiac pulse signal (P. Leonard et al. 2003; Paul Leonard et al. 2004; P. A. Leonard et al. 2006; Shelley et al. 2006; Charlton et al. 2018). Chon et al. (Chon, Dash, y Ju 2009) proposed a method to estimate respiratory rate by pulse oximetry using the time-frequency spectral estimation method: variable frequency complex demodulation (VCFDM) to identify the frequency modulation (FM and AM) of the photoplethysmogram waveform.

The photoplethysmography technique is widely known and a wide range of technologies have been developed around it (Kyriacou y Allen 2021). One of the main reasons for using this technique is to avoid the use of additional equipment in monitoring vital signs such as heart rate or respiratory rate (Addison y Watson 2004). It is important to know the range of beats per minute and breaths per minute at rest and during exercise; for example, the respiratory rate range is between 10-20 breaths/minute and can reach up to 45 breaths/minute for sports activities, and in the case of heart rate, it is between 38 and 110 beats/minute, including sports activities (Nakajima, Tamura, y Miike 1996). Knowledge of these ranges allows us to design the electronic system, mainly the noise-reducing filters in the signal to capture the cardiac pulse signal or respiratory rate signal that is in these ranges (Budidha y Kyriacou

2022). Currently, existing technology makes possible the evolution of conventional PPG to image PPG (IPPG) (Sun y Thakor 2016), algorithms based on four-layer deep neural networks (Biswas et al. 2019) are also being applied, indicating that it is still a field with numerous research possibilities. Based on the pulse oximetry setup and Ohmeda oximeter review by Wukitsch et al. (Wukitsch et al. 1988), we propose to generate a train of pulses in such a way that for a time the red LED remains on and the infrared LED off, and vice versa, synchronizing by a signal from a microcontroller. For the proposed case, both light beams are used under the principle that the recovered signal is amplitude modulated (AM) by the heart rate. The heart rate signal is recovered by applying the synchronous demodulation technique to the signal from the photodetector.

The demodulation technique has been widely used since its origin in the field of communications (Bruning et al. 1974), but it is also used in other research areas such as optics (Malacara 2007; Rodríguez-Vera y Servín 1994; Servin, Malacara, y Rodriguez-Vera 1994). Instruments have been developed specifically for its implementation (Zurich Instruments 2016). The synchronous detection technique requires that the input signal to meet specific requirements: be purely sinusoidal and have a duty cycle of at least 0.5 in order to determine the phase and amplitude of an input signal at a given frequency (Warsza 2005). The signal can be analyzed by electronic or digital procedures; the photoplethysmography technique allows the signal to be analyzed by a digital procedure, although extensive instrumentation (technology) has already been developed (Kyriacou y Allen 2021). In the synchronous detection section, the procedure used is discussed more extensively. A procedure for applying synchronous detection in the detection of pulsed signals can be found in (Efthymiou y Ozanyan 2013), where they show us a periodic signal with a duty cycle close to 0.5, this signal is improved by data processing using a Gated Quadrature Synchronous Demodulation (GQSD) algorithm to achieve optimal pulse recovery conditions.

This article is divided into the following sections. The introduction presents the state of the art, theoretical framework and the proposal. In the development section, the operating principle is presented, together with the mathematical demonstration of the theory on which the method for the treatment and recovery of the heart rate signal is based. The results section shows the theory described in the development applied to practice and the graphs (Fig. 6 and Fig. 7) show the signal before and after applying the synchronous detection method to the collected data from the signal acquisition system. In the conclusions, the final argument for the synchronous detection method and the possible implementation in future works for recovering other signals immersed in the photoplethysmography signal are presented.

METHODOLOGÝ

Methods and procedures

Participant Information: The initial trials of the technique were conducted with two participants to establish its feasibility. More participants will be included in future studies. In total, 100 measurements were collected from two subjects, each of whom was evaluated 50 times. The subject characteristics are as described in the article by Fine et al. (Fine et al. 2021) they analyze the sources of noise in photoplethysmography (PPG) and their impact on the development of PPG devices for health monitoring. In their analysis, they discuss the reduced accuracy of PPG devices using green light (550 nm) in individuals with darker skin tones due to melanin absorption in the epidermis.

Red light and near-infrared light, with their ability to penetrate deeper into the skin, offer better performance in such cases. Some of the subject characteristics are shown below.

Subject 1

Age: Thirty-seven years old

Sex: Female

Physical condition: Active

Medications: None

Skin tone: Brown

Build: Thin

Measurement site: Index finger

Body temperature: 36.5 degrees Celsius

Subject 2

Age: Fifty-four years old

Sex: Male

Physical condition: Active

Medications: None

Skin tone: Brown

Build: Thin

Measurement site: Index finger

Body temperature: 36.5 degrees Celsius

Principle of Operation: Fig. 1 provides a basic flow diagram of the circuit designed for data collection. The PIC16F1615 microprocessor, through the pulse width modulation (PWM) function, generated a pulse train at a frequency of 122 Hz.

Figure 1

Basic diagram of the circuit used for data collection

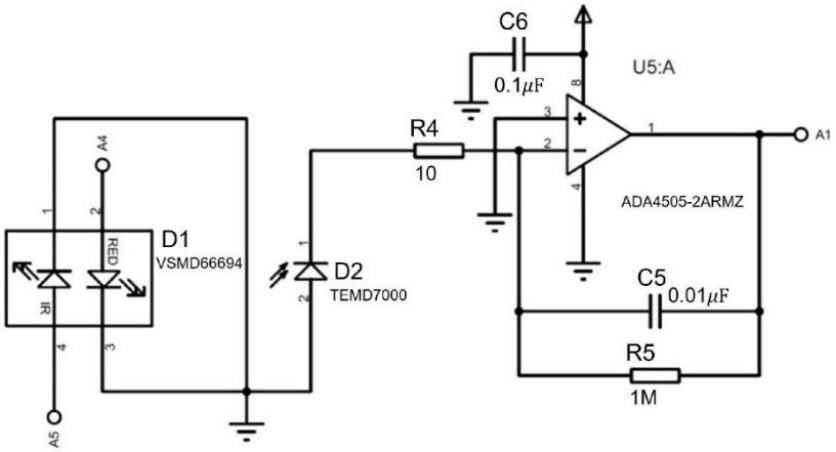

The same microprocessor controlled an on–and–off system of red and infrared LEDs (VSMD66694). This control allowed one LED to remain on for a period of 8 pulses (data sampling period and its storage in memory) while the other remained off, and vice versa (Fig. 2). The emission of the beams interacts with the surface of human skin. The reflected light was collected and processed by the TEMD7000 photo-detector which is connected to a transimpedance circuit whose main component is the ADA4505-2ARMZ amplifier, the output signal of the transimpedance circuit is amplified to become a digital signal. The processor sends the data to the CY15V104QN 4 Mbit F-RAM memory. The time for sending the signal (pulse train), collecting and storing data lasts 133 seconds (2.13 minutes). The signal sampling frequency was 1950 Hz (t = 5.12x10−4 seconds). Once the data was stored, the circuit was connected to a computer to extract the data through the USB port, the data was analyzed by the synchronous demodulation algorithm which was programmed in the Python programming language.

The configuration of the analogue system used is shown in Fig. 2.

Figure 2

Basic connection diagram for the analogue data collection system, where ir is an infrared LED, r is a red LED, R is the resistance, Op is the operational amplifier and GND is a ground line

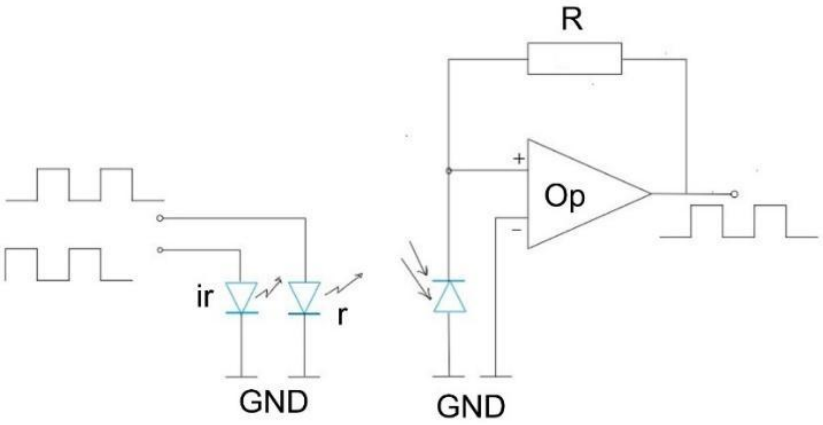

Signal processing method: The procedure for the implementation of the synchronous demodulation algorithm is summarized next:

A train of pulses is sent to interact with the skin, Fig. 3.

The signal collected by the photodetector is taken, which has already gone through an analog and digital conditioning process.

Apply a low-pass filter to the signal.

The frequency of the input signal is calculated.

With the frequency of the input signal, two signals are generated: sine and cosine.

A convolution is applied between the input signal and the sine and cosine signal respectively; this generates two signals.

Apply a low-pass filter to the signal.

Feature scaling (normalization) is applied to the signal data generated in the previous step.

A low-pass filter is applied to the signals resulting from the previous step.

Finally, the magnitude of these two signals is calculated, which corresponds to the heart pulse rate.

Figure 3

Pulse train: on-and-off sequence for the LEDs. The pulse train frequency is 122 Hz. It is important to note that there is a dead time in neither of the two LEDs are on to avoid data overlap, this time is 500 ns

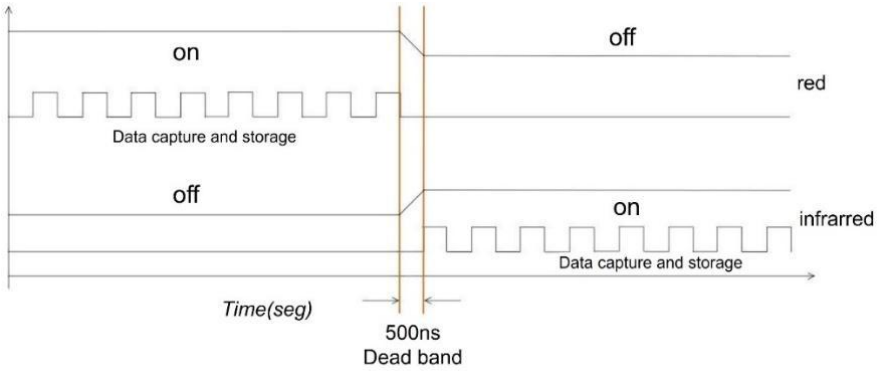

The following equation describes a pulse train (Poularikas 2010):

$$t_p = sgn(cos\ cos\ (2\pi ft)\ ) = sgn(cos\ cos\ (\omega t)\ ) \quad (1)$$

For this case, a pulse train is applied that is defined by the following form:

$$t_p = sgn(cos\ cos\ (2\pi ft)\ ) = A + sgn(cos\ cos\ (\omega t)\ ) \quad (2)$$

Where t_p is the pulse train function, t is time, f is the fundamental frequency and A is a constant.

Photoplethysmography (Allen 2007; Mendelson y Ochs 1988; Nakajima, Tamura, y Miike 1996) is a technique that allows visualizing the variation in blood volume changes as a result of flow variations, thus allowing the detection and measurement of cardiac pulse, oxygen levels, and other biomedical variables (Karlen et al. 2013). Herein, plethysmography is used to measure heart rate. The light beams were applied in the form of a pulse train, as indicated by Equation (2). The signal was recovered by reflection. If a convolution low-pass filter is applied to the sampled signal (Stearns y Hush 2011), the following is obtained:

$$x(t) = \left[t_p(t)\right] * F_{pb} = A + B\ cos\ cos\ \left(\omega_p t\right)\ = A + B\ cos\ cos\ \left(2\pi f_p t\right) \tag{3}$$

where $\omega p\ =\ 2\pi fp$, where ω_p is the angular frequency of the carrier signal. From Equation (3) it can be seen that there is a constant component A that corresponds to an unchanged illumination beam and that its magnitude is much greater than the amplitude of the oscillating signal $|A|\ \gg\ |B|$. Fig. 4 shows the signal recovered from the data acquisition system after applying a low-pass filter, as mentioned in step 3 of the implementation of the synchronous demodulation algorithm, and Fig. 5 shows the Fourier spectrum of the oscillation frequency of both light beams (122 Hz).

Graphic 1

Signal recovered by the sensor due to the light (red and infrared LEDs) reflected on the incident surface

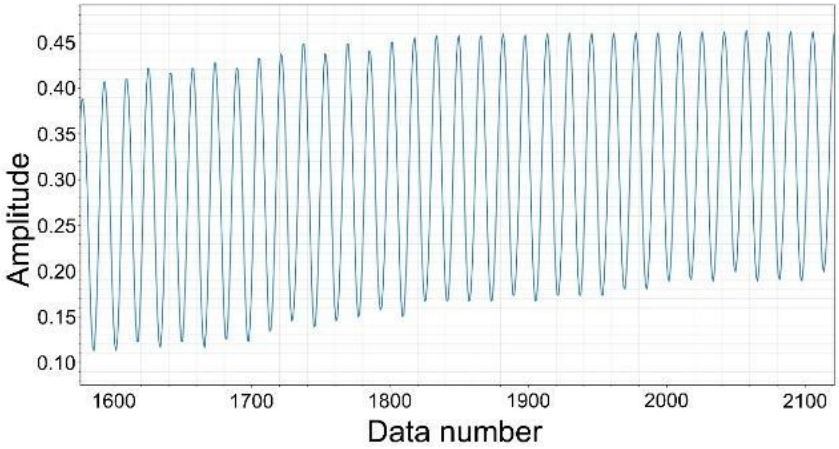

Graphic 2

Frequency of oscillation of red and infrared LEDs

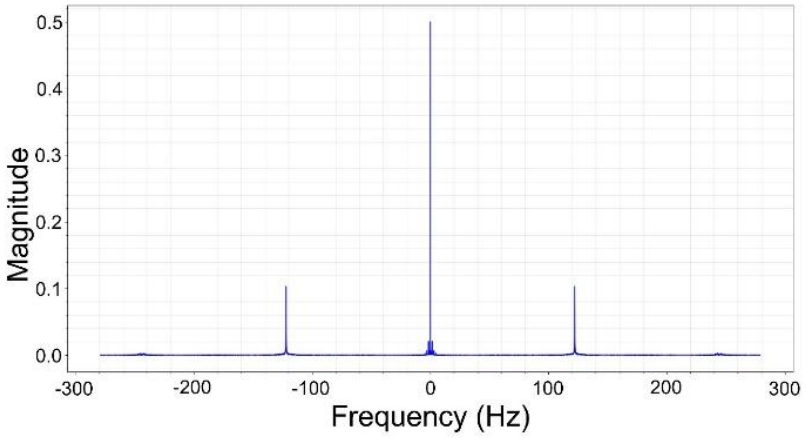

Synchronous detection: The synchronous detection(Malacara 2007) method is based on the theory of radio communication, where the phase or magnitude of an unknown signal is recovered by the correlation of this signal with a sinusoidal signal of the same frequency (Rodríguez-Vera y Servín 1994). If we consider that the signal derived from the heart rate, denoted as ($|P(t)|$), can modulate a train of pulses according to Equation (2), with a carrier frequency ($fp, p: carrier$) much higher than the frequency of heart rate ($fr, r: heart\ rate$) and we can consider this signal as a carrier signal. Therefore:

$$f_r \ll f_p \tag{4}$$

A relationship can be considered as follows:

$$y(t) = P(t)x(t) = P(t)\left[A + B\ cos\ cos\ \left(2\pi f_p t\right)\right] \tag{5}$$

From Equation (5), we have the following:

$$y(t) = AP(t) + BP(t)\ cos\ cos\ \left(2\pi f_p t\right)$$

Knowing that $|A| \gg |P(t)|$ and also that $|P(t)|$ will only modulate the $B\ cos(2\pi fpt)$. If this signal ratio shown in equation (5) is multiplied by 2 signals (sine and cosine) of frequency similar to the carrier frequency, the following is obtained. If this signal ratio shown in equation (5) is multipliedby 2 signals (sine and cosine) of frequency similar to the carrier frequency, the following is obtained.

$$y(t)\ cos\ cos\ \left(2\pi f_p, t\right) = P(t)\left[A + B\ cos\ cos\ \left(2\pi f_p t\right)\right] cos\ cos\ \left(2\pi f_p, t\right)$$

If the previous expression is developed, the Equation (6) is obtained:

$$y(t)\ cos\ cos\ \left(2\pi f_p, t\right) = AP(t)\ cos\ cos\ \left(2\pi f_p, t\right) + BP(t)\ cos\ cos\ \left(2\pi f_p t\right)\ cos\ cos\ \left(2\pi f_p, t\right) \tag{6}$$

A similar analysis is applied for the following relationship:

$$y(t)\ sin\ sin\ (2\pi f_p,t)\ = P(t)[A + B\ cos\ cos\ (2\pi f_p t)\ ]\ sin\ sin\ (2\pi f_p,t)$$

From the previous analysis we obtain Equation (7):

$$y(t)\ sin\ sin\ (2\pi f_p,t)\ = AP(t)\ sin\ sin\ (2\pi f_p,t)\ + BP(t)\ cos\ cos\ (2\pi f_p t)\ \ sin\ sin\ (2\pi f_p,t) \quad (7)$$

Equation (6) can be expressed as follows:

$$y(t)\ cos\ cos\ (2\pi f_p,t)\ = S_{DC_{cos}} + S_{AC_{cos}} = y(t)_c \quad (8)$$

Where:

$$S_{DC_{cos}} = \ AP(t)\ cos\ cos\ (2\pi f_p,t)$$
$$S_{AC_{cos}} = BP(t)\ cos\ cos\ (2\pi f_p t)\ \ cos\ cos\ (2\pi f_p,t)$$

Equation (7) is also expressed as follows:

$$y(t)\ sin\ sin\ (2\pi f_p,t)\ = S_{DC_{sin}} + S_{AC_{sin}} = y(t)_s \quad (9)$$

Where:

$$S_{DC_{sin}} = \ AP(t)\ sin\ sin\ (2\pi f_p,t)$$
$$S_{AC_{sin}} = BP(t)\ cos\ cos\ (2\pi f_p t)\ \ sin\ sin\ (2\pi f_p,t)$$

$S_{AC_{cos}}$ and $S_{AC_{sin}}$ are the terms containing the information of interest, for cardiac pulse recovery. To apply the synchronous demodulation technique, the term containing the constant A ($S_{DC_{cos}}$ and $S_{DC_{sin}}$) must be removed from Equation (6) and (7) respectively to subsequently process the terms of interest ($S_{AC_{cos}}$ and $S_{AC_{cos}}$). For this purpose, we normalize y(t)c and y(t)s from Equations (8) and (9) as follows:

From the previous mathematical development, we obtain the signals of Equation (8) and (9), both signals carry a DC component and we can rewrite the equations as shown:

$$y(t)_c = y(t)\ cos\ cos\ (2\pi f_p,t)\ = S_{DC_{cos}} + S_{AC_{cos}} \quad (10)$$

$$y(t)_s = y(t)\ sin\ sin\ (2\pi f_p,t)\ = S_{DC_{sin}} + S_{AC_{sin}} \quad (11)$$

Before applying feature scaling, both signals ($S_{DC_{cos}}$) and $S_{DC_{sin}}$) of equations (10) and (11) are processed by applying a low-pass filter; The DC signal is attenuated with the application of the low pass filter, however, it is not completely removed, so the next step is to apply the following statistical procedure known as feature scaling to remove by the DC signal. This normalization consists of transforming the minimum value into 0 and the maximum value into 1 so that all other values remain within that range (to meet the signal characteristics mentioned in Zygmunt L. Warsza's publication in the handbook of measuring system design manual (Warsza 2005), the formula is as follows:

$$N_{min-max} = \frac{f - min}{- min} \quad (12)$$

Where: f = is the signal of $y(t)_c$ and $y(t)_s$, because both signals must be normalized.

Equation (12) returns values between 0 and 1, which needs to be corrected as it requires a signal centered on the x-axis or located between values above and below 0, with a minimum amplitude of 0.5 (Efthymiou y Ozanyan 2013), for this purpose Z − score normalization is used which is defined by the following Equation (13):

$$y(t)_{NC} = \frac{N_{min-max} - \mu}{\sigma} \tag{13}$$

Where:

$N_{min-max}$= Are the data obtained from Equation (12).

μ = It is the Arithmetic Average $N_{min-max}$

σ = Is the Standard Deviation of $N_{min-max}$

In Z - score normalization if a value is exactly equal to the mean of the data, this value is normalized to 0; if the value is below the mean, then it will be transformed to a negative number, and if the value is above the mean, the value is transformed to a positive value. In Z - score normalization the amplitude of the signal is determined by the standard deviation of the data. The data resulting from Z - score normalization, are the signals $y(t)_{NC}$ and $y(t)_{NS}$:

$$y(t)_{NC} = P(t)\ cos\ cos\ (2\pi f_{p'}t)\ + BP(t)\ cos\ cos\ (2\pi f_p t)\ cos\ cos\ (2\pi f_{p'}t) \tag{14}$$
$$y(t)_{NS} = P(t)\ sin\ sin\ (2\pi f_{p'}t)\ + BP(t)\ sin\ sin\ (2\pi f_p t)\ sin\ sin\ (2\pi f_{p'}t) \tag{15}$$

From equation (14) and (15) note that the A term is no longer present, since it is centered with respect to the time axis.

If we develop the $S_{AC_{cos}}$ part of Equation (14), we obtain the following:

$$\begin{aligned} &BP(t)\ cos\ cos\ (2\pi f_p t)\ cos\ cos\ (2\pi f_{p'}t) \\ &\quad = BP(t)\left[\frac{1}{2}cos\ cos\ (2\pi(f_p - f_{p'})t)\ + \frac{1}{2}cos\ cos\ (2\pi(f_p + f_{p'})t)\right] \\ &\quad = (2\pi(f_p - f_{p'})t)\ + B'P(t)\ cos\ cos\ (2\pi(f_p + f_{p'})t) \\ &\quad = B'P(t)[cos\ cos\ (2\pi(f_p - f_{p'})t)\ + cos\ cos\ (2\pi(f_p + f_{p'})t)\ ] \end{aligned}$$

Developing the $S_{AC_{sin}}$ part of Equation (15), we obtain the following:

$$\begin{aligned} &BP(t)\ cos\ cos\ (2\pi f_p t)\ sin\ sin\ (2\pi f_{p'}t) \\ &\quad = BP(t)\left[\frac{1}{2}sin\ sin\ (2\pi(f_p - f_{p'})t)\ + \frac{1}{2}sin\ sin\ (2\pi(f_p + f_{p'})t)\right] \\ &\quad = (2\pi(f_p - f_{p'})t)\ + B'P(t)\ sin\ sin\ (2\pi(f_p + f_{p'})t) \\ &\quad = B'P(t)[sin\ sin\ (2\pi(f_p - f_{p'})t)\ + sin\ sin\ (2\pi(f_p + f_{p'})t)\ ] \end{aligned}$$

Where $B' = \frac{B}{2}$

Fig. 6 shows the signal coming from the data acquisition system after having applied a low-pass filter according to Equation (3), it can be seen how the heart rate modulates the signal. Therefore, Equations (14) and (15) can be rewritten as follows:

$$y(t)_c = P(t)\, cos\, cos\, (2\pi f_{p\prime} t) \; + \; B'P(t)[cos\, cos\, (2\pi(f_p - f_{p\prime})t) \; + cos\, cos\, (2\pi(f_p + f_{p\prime})t)\,] \qquad (16)$$

$$y(t)_s = P(t)\, sin\, sin\, (2\pi f_{p\prime} t) \; + \; B'P(t)[sin\, sin\, (2\pi(f_p - f_{p\prime})t) \; + sin\, sin\, (2\pi(f_p + f_{p\prime})t)\,] \qquad (17)$$

The terms $cos\, cos\, \left(2\pi\left(f_p - f_{p'}\right)t\right)$ and $sin\, sin\, \left(2\pi\left(f_p - f_{p'}\right)t\right)$ corresponds to low frequency, and the terms $cos\, cos\, \left(2\pi f_{p'}t\right)$, $sin\, sin\, \left(2\pi f_{p'}t\right)$, $cos\, cos\, \left(2\pi\left(f_p + f_{p'}\right)t\right)$ and $sin\, sin\, \left(2\pi\left(f_p + f_{p'}\right)t\right)$ corresponds to high frequencies, if it is considered that $fr \ll fp$.

By applying a low-pass filter (Butterworth type [33]) to the Equation (16) and (17), the following is obtained:

$$f_c = y(t)_c * F_{pb} = \; B'P(t)\, cos\, cos\, (2\pi(f_p - f_{p\prime})t) \qquad (18)$$

In addition, if $f_{p\prime} \approx f_p$, and after applying a low-pass filter, then:

$$f_s = y(t)_s * F_{pb} = \; B'P(t)\, sin\, sin\, (2\pi(f_p - f_{p\prime})t) \qquad (19)$$

It is not interesting to recover the phase but rather the magnitude of ($|P(t)|$), because the signal from the photodetector is amplitude modulated (AM) by the heart rate. From the previous Equations (18) and (19), the following is obtained:

$$|P(t)| = \sqrt{('P(t)\, cos\, cos\, (2\pi(f_p - f_{p\prime})t)\,)^2 + (B'P(t)\, sin\, sin\, (2\pi(f_p - f_{p\prime})t)\,)^2}$$

Therefore, we have the following:

$$|P(t)| = \sqrt{(f_c)^2 + (f_s)^2} \qquad (20)$$

From Equation (20), heart rate is calculated.

Graphic 3

Recovered signal to which the low-pass filter has been applied according to Equation (3)

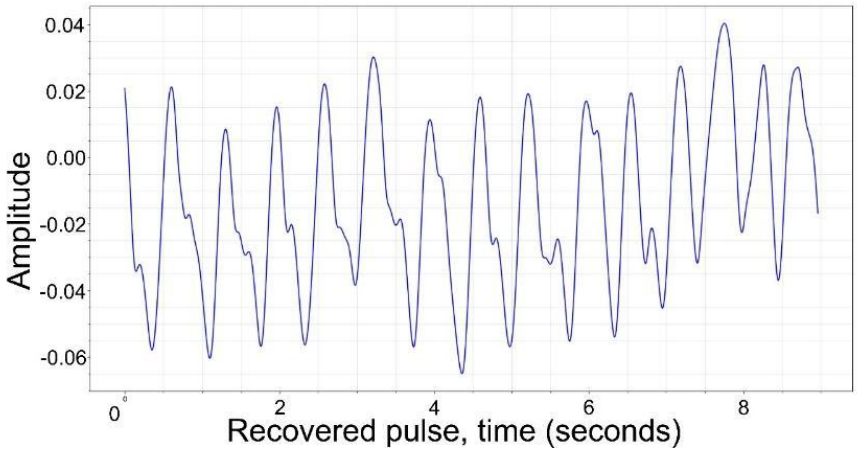

RESULTS

Applying the described procedure, the following results are obtained: Fig. 6 shows the processed signal that is obtained from the signal acquisition system, that is, after Equation (3) is applied.

Applying the procedure according to Equations (18), (19) and (20), the result is shown in graphic 3 is obtained.

Graphic 4

Pulse recovered from the synchronous detection method

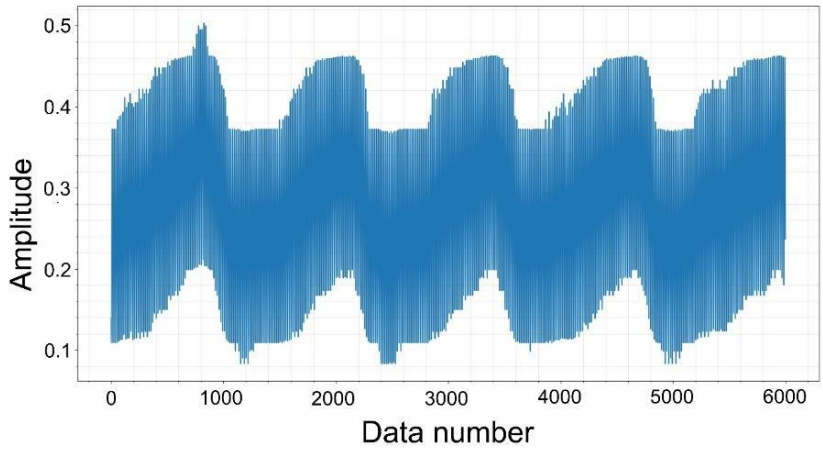

Graphic 4 shows the signal of interest recovered with the pulse oximetry technique in conjunction with the synchronous demodulation technique: heart rate. It is also observed that the pulse signal is modulated by an additional signal. Applying the Fourier transform to the data obtained, the following frequency spectrum is obtained (graphic 5).

Graphic 5

Fourier spectrum of the data obtained by applying the synchronous detection method

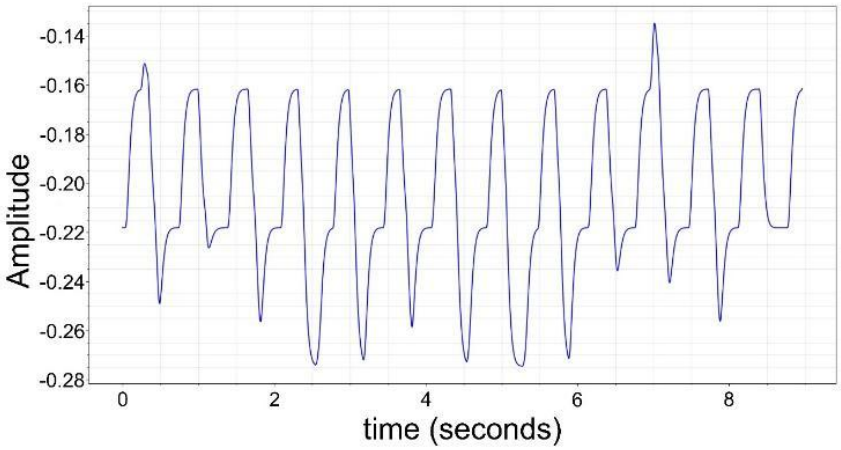

The main peaks are at a frequency of 1.5p/s, which is corroborated by the signal in graphic 6, $\frac{14p}{9s} = 1.5p/s$ (pulses per second). Other important aspects to highlight are the peaks between the origin and the heart rate, which were studied by Solange et al. (Akselrod et al. 1981).

The data, which are obtained using the photoplethysmography technique, are shown in graphic 6.

Graphic 6

Data results from directly applying the photoplethysmography method

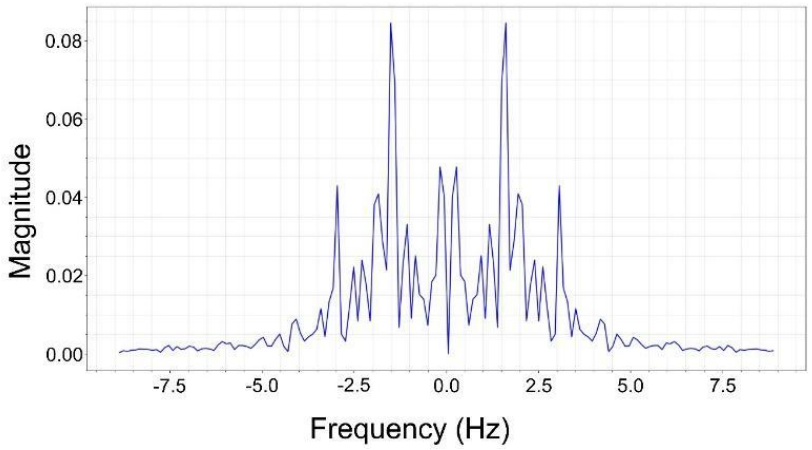

Their respective frequency spectrum can be seen in graphic 7.

Graphic 7

Fourier spectrum of the photoplethysmography method data

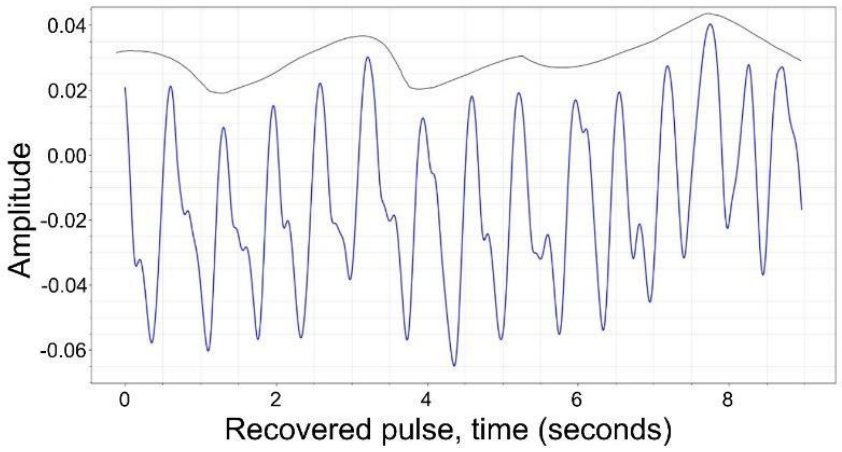

The frequency corresponding to the data applying the synchronous detection method corresponds to that of the data obtained directly applying the photoplethysmography technique $f = 1.5p/s$.

From the data obtained with the proposed method (graphic 7), it can be seen that the pulse is modulated; therefore, it is possible to apply techniques that can determine the respiratory rate (P. Leonard et al. 2003; Paul Leonard et al. 2004; P. A. Leonard et al. 2006; Shelley et al. 2006; Charlton et al. 2018) (graphic 8).

Graphic 8

Heart rate modulated by lung rate

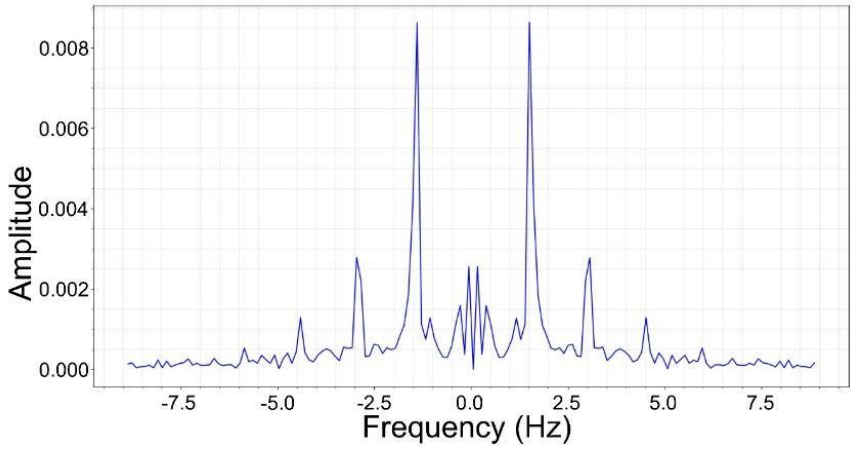

The peaks of each spectrum and the measurement obtained with the MD300C23 CHOICEMED pulse oximeter are shown in Table 1.

Table 1

Mean squared error of the peaks in the heart rate frequency spectrum

number of observations	Subject 1			Subject 2		
	Estimated spectrum frequency data	Observed CHOICEMED pulse oximeter data	Sum of the squared errors	Estimated spectrum frequency data	Observed CHOICEMED pulse oximeter data	Sum of the squared errors
1	67	69	4	65	67	4
2	78	79	1	63	64	1
3	71	72	1	69	67	4
4	63	65	4	68	70	4
5	57	54	9	61	63	4
6	72	70	4	63	65	4
7	64	65	1	60	58	4
8	85	84	1	70	71	1
9	61	63	4	67	68	1
10	56	57	1	65	67	4
11	70	70	0	62	65	9
12	65	64	1	64	63	1
13	86	85	1	63	62	1
14	85	87	4	70	73	9
15	66	70	16	65	63	4
16	76	73	9	70	71	1
17	105	107	4	62	61	1
18	95	99	16	63	62	1
19	79	75	16	63	61	4
20	85	86	1	66	70	16
21	66	69	9	64	67	9
22	85	87	4	61	59	4
23	70	73	9	77	75	4
24	89	94	25	62	66	16
25	67	66	1	67	65	4
26	75	77	4	68	67	1
27	74	72	4	69	72	9
28	80	79	1	68	69	1
29	64	66	4	67	68	1
30	91	89	4	67	69	4
31	82	79	9	60	58	4
32	81	85	16	65	62	9
33	87	88	1	60	59	1
34	88	90	4	61	62	1
35	87	85	4	65	67	4
36	68	65	9	70	68	4
37	66	69	9	72	70	4
38	83	80	9	60	63	9
39	86	87	1	68	67	1
40	62	64	4	55	58	9
41	80	79	1	65	66	1
42	85	86	1	61	62	1
43	77	78	1	54	57	9
44	68	70	4	63	62	1
45	80	82	4	65	63	4
46	86	88	4	66	69	9

47	85	84	1	67	65	4
48	83	84	1	65	62	9
49	58	60	4	60	64	16
50	87	89	4	54	57	9
average	76.52	77.16	5.08	64.5	64.98	4.8

CONCLUSION

Plethysmography is a technique that has a wide application in the clinical field. Its implementation has allowed the development of a new technology, as well as a new technique in the treatment of data for scrutinizing the additional information carried by the cardiac pulse signal. The application of the synchronous detection method was presented as a technique to recover the cardiac pulse through the configuration used in pulse oximetry. From the results obtained, the cardiac pulse recovered from the set of information generated by the pulse oximeter configuration at two different wavelengths is shown. In addition, cardiac pulse modulation can be achieved, which can guide the application of pulmonary rate recovery techniques.

REFERENCES

Addison, Paul S., y James N. Watson. 2004. «Secondary transform decoupling of shifted nonstationary signal modulation components: application to photoplethysmography». International Journal of Wavelets, Multiresolution and Information Processing 02 (01): 43-57. https://doi.org/10.1142/S0219691304000329.

Akselrod, S., D. Gordon, F. A. Ubel, D. C. Shannon, A. C. Berger, y R. J. Cohen. 1981. «Power Spectrum Analysis of Heart Rate Fluctuation: A Quantitative Probe of Beat-to-Beat Cardiovascular Control». Science (New York, N.Y.) 213 (4504): 220-22. https://doi.org/10.1126/science.6166045.

Allen, John. 2007. «Photoplethysmography and Its Application in Clinical Physiological Measurement». Physiological Measurement 28 (3): R1-39. https://doi.org/10.1088/0967-3334/28/3/R01.

Anderson, R. Rox, y John A. Parrish. 1981. «The Optics of Human Skin». Journal of Investigative Dermatology 77 (1): 13-19. https://doi.org/10.1111/1523-1747.ep12479191.

Biswas, Dwaipayan, Luke Everson, Muqing Liu, Madhuri Panwar, Bram-Ernst Verhoef, Shrishail Patki, Chris H. Kim, et al. 2019. «CorNET: Deep Learning Framework for PPG-Based Heart Rate Estimation and Biometric Identification in Ambulant Environment». IEEE Transactions on Biomedical Circuits and Systems 13 (2): 282-91. https://doi.org/10.1109/TBCAS.2019.2892297.

Bruning, J. H., D. R. Herriott, J. E. Gallagher, D. P. Rosenfeld, A. D. White, y D. J. Brangaccio. 1974. «Digital Wavefront Measuring Interferometer for Testing Optical Surfaces and Lenses». Applied Optics 13 (11): 2693-2703. https://doi.org/10.1364/AO.13.002693.

Budidha, Karthik, y Panicos Kyriacou. 2022. «Photoplethysmography technology». En , 43-68. https://doi.org/10.1016/B978-0-12-823374-0.00002-5.

Challoner, A. V., y C. A. Ramsay. 1974. «A Photoelectric Plethysmograph for the Measurement of Cutaneous Blood Flow». Physics in Medicine and Biology 19 (3): 317-28. https://doi.org/10.1088/0031-9155/19/3/003.

Chan, Edward D., Michael M. Chan, y Mallory M. Chan. 2013. «Pulse Oximetry: Understanding Its Basic Principles Facilitates Appreciation of Its Limitations». Respiratory Medicine 107 (6): 789-99. https://doi.org/10.1016/j.rmed.2013.02.004.

Charlton, Peter H., Drew A. Birrenkott, Timothy Bonnici, Marco A. F. Pimentel, Alistair E. W. Johnson, Jordi Alastruey, Lionel Tarassenko, Peter J. Watkinson, Richard Beale, y David A. Clifton. 2018. «Breathing Rate Estimation From the Electrocardiogram and Photoplethysmogram: A Review». IEEE Reviews in Biomedical Engineering 11: 2-20. https://doi.org/10.1109/RBME.2017.2763681.

Chon, Ki H., Shishir Dash, y Kihwan Ju. 2009. «Estimation of Respiratory Rate from Photoplethysmogram Data Using Time-Frequency Spectral Estimation». IEEE Transactions on Bio-Medical Engineering 56 (8): 2054-63. https://doi.org/10.1109/TBME.2009.2019766.

Efthymiou, Spyros, y Krikor B. Ozanyan. 2013. «Pulse Detection by Gated Synchronous Demodulation». IEEE Sensors Journal 13 (9): 3349-60. https://doi.org/10.1109/JSEN.2013.2263496.

Fine, Jesse, Kimberly L. Branan, Andres J. Rodriguez, Tananant Boonya-ananta, Ajmal, Jessica C. Ramella-Roman, Michael J. McShane, y Gerard L. Coté. 2021. «Sources of Inaccuracy in Photoplethysmography for Continuous Cardiovascular Monitoring». Biosensors 11 (4): 126. https://doi.org/10.3390/bios11040126.

Hertzman, Alrick B. 1938. «The blood supply of various skin areas as estimated by the photoelectric plethysmograph». American Journal of Physiology-Legacy Content 124 (2): 328-40. https://doi.org/10.1152/ajplegacy.1938.124.2.328.

Karlen, Walter, Srinivas Raman, J. Mark Ansermino, y Guy A. Dumont. 2013. «Multiparameter Respiratory Rate Estimation from the Photoplethysmogram». IEEE Transactions on Bio-Medical Engineering 60 (7): 1946-53. https://doi.org/10.1109/TBME.2013.2246160.

Kock, J. P. de, y L. Tarassenko. 1993. «Pulse Oximetry: Theoretical and Experimental Models». Medical and Biological Engineering and Computing 31 (3): 291-300. https://doi.org/10.1007/BF02458049.

Kyriacou, Panicos, y John Allen. 2021. Photoplethysmography - Technology, Signal Analysis and Applications. 1st Edition. © Academic Press 2021. https://www.elsevier.com/books/photoplethysmography/kyriacou/978-0-12-823374-0.

Leonard, P., T. F. Beattie, P. S. Addison, y J. N. Watson. 2003. «Standard Pulse Oximeters Can Be Used to Monitor Respiratory Rate». Emergency Medicine Journal: EMJ 20 (6): 524-25. https://doi.org/10.1136/emj.20.6.524.

Leonard, Paul A., David Clifton, Paul S. Addison, James N. Watson, y Tom Beattie. 2006. «An Automated Algorithm for Determining Respiratory Rate by Photoplethysmogram in Children». Acta Paediatrica (Oslo, Norway: 1992) 95 (9): 1124-28. https://doi.org/10.1080/08035250600612280.

Leonard, Paul, Neil R. Grubb, Paul S. Addison, David Clifton, y James N. Watson. 2004. «An Algorithm for the Detection of Individual Breaths from the Pulse Oximeter Waveform». Journal of Clinical Monitoring and Computing 18 (5-6): 309-12. https://doi.org/10.1007/s10877-005-2697-z.

Leppänen, Timo, Samu Kainulainen, Henri Korkalainen, Saara Sillanmäki, Antti Kulkas, Juha Töyräs, y Sami Nikkonen. 2022. «Pulse Oximetry: The Working Principle, Signal Formation, and Applications». En Advances in the Diagnosis and Treatment of Sleep Apnea : Filling the Gap Between Physicians and Engineers, editado por Thomas Penzel y Roberto Hornero, 205-18. Cham: Springer International Publishing. https://doi.org/10.1007/978-3-031-06413-5_12.

Loh, H. W., S. Xu, O. Faust, C. P. Ooi, P. D. Barua, S. Chakraborty, R.-S. Tan, F. Molinari, y U. R. Acharya. 2022. «Application of Photoplethysmography Signals for Healthcare Systems: An in-Depth Review.», abril. https://opus.lib.uts.edu.au/handle/10453/167716.

Malacara, Daniel, ed. 2007. Optical Shop Testing. 3rd ed. Wiley Series in Pure and Applied Optics. Hoboken, N.J: Wiley-Interscience.

Mendelson, Yitzhak, y B.D. Ochs. 1988. «Noninvasive pulse oximetry utilizing skin reflectance photoplethysmography». IEEE Transactions on Biomedical Engineering 35 (10): 798-805. https://doi.org/10.1109/10.7286.

Nakajima, K., T. Tamura, y H. Miike. 1996. «Monitoring of Heart and Respiratory Rates by Photoplethysmography Using a Digital Filtering Technique». Medical Engineering & Physics 18 (5): 365-72. https://doi.org/10.1016/1350-4533(95)00066-6.

Poularikas, Alexander D., ed. 2010. Transforms and Applications Handbook. 3rd ed. Electrical Engineering Handbook ; 43. Boca Raton, Fla: CRC Press.

Rodríguez-Vera, R., y M. Servín. 1994. «Phase Locked Loop Profilometry». Optics & Laser Technology 26 (6): 393-98. https://doi.org/10.1016/0030-3992(94)90050-7.

Servin, M., D. Malacara, y R. Rodriguez-Vera. 1994. «Phase-Locked-Loop Interferometry Applied to Aspheric Testing with a Computer-Stored Compensator». Applied Optics 33 (13): 2589-95. https://doi.org/10.1364/AO.33.002589.

Shelley, Kirk H., Aymen A. Awad, Robert G. Stout, y David G. Silverman. 2006. «The Use of Joint Time Frequency Analysis to Quantify the Effect of Ventilation on the Pulse Oximeter Waveform». Journal of Clinical Monitoring and Computing 20 (2): 81-87. https://doi.org/10.1007/s10877-006-9010-7.

Stearns, Samuel D., y Donald R. Hush. 2011. Digital Signal Processing with Examples in MATLAB(R). 2nd ed. Boca Raton, FL.

Sun, Yu, y Nitish Thakor. 2016. «Photoplethysmography revisited: from contact to noncontact, from point to imaging». IEEE transactions on bio-medical engineering 63 (3): 463-77. https://doi.org/10.1109/TBME.2015.2476337.

Warsza, Zygmunt. 2005. Handbook of Measuring System Design, 3 Volume Set | Wiley. Vol. 3.

Wukitsch, Michael W., Michael T. Petterson, David R. Tobler, y Jonas A. Pologe. 1988. «Pulse Oximetry: Analysis of Theory, Technology, and Practice». Journal of Clinical Monitoring 4 (4): 290-301. https://doi.org/10.1007/BF01617328.

Zurich Instruments. 2016. «Principles of Lock-in Detection and the State of the Art». Zurich Instruments. noviembre de 2016. https://www.zhinst.com/americas/en.

ACKNOWLEDGMENT

We thank CONACYT for the support for the development of research project 287237: Physiological and behavioural responses of blue abalone (Haliotis fulgens, Philippi 1845), under thermal stress, by hypoxia and simultaneous effect: evaluation by physiology, biochemistry and optoelectronics, from which this work was derived.